Theoretical Study on the Reaction Mechanism of VO_2^+ with Propyne in Gas Phase

Lourdes Gracia,[†] Victor Polo,[†] Julio R. Sambrano,[‡] and Juan Andrés*,[†]

Departament de Química Física i Analítica, Universitat Jaume I, Box 224, 12080 Castelló, Spain, and Grupo de Modelagem e Simulação Molecular, DM, Unesp, Universidade Estadual, Paulista, Box 473, 17033-360 Bauru, Brazil

Received: November 16, 2007; In Final Form: December 19, 2007

Possible molecular mechanisms of the gas-phase ion/molecule reaction of VO_2^+ in its lowest singlet and triplet states ($^1A_1/^3A''$) with propyne have been investigated theoretically by density functional theory (DFT) methods. The geometries, energetic values, and bonding features of all stationary and intersystem crossing points involved in the five different reaction pathways (paths 1−5), in both high-spin (triplet) and low-spin (singlet) surfaces, are reported and analyzed. The oxidation reaction starts by a hydrogen transfer from propyne molecule to the vanadyl complex, followed by oxygen migration to the hydrocarbon moiety. A hydride transfer process to the vanadium atom opens four different reaction courses, paths 1−4, while path 5 arises from a hydrogen transfer process to the hydroxyl group. Five crossing points between high- and low-spin states are found: one of them takes place before the first branching point, while the others occur along path 1. Four different exit channels are found: elimination of hydrogen molecule to yield propynaldehyde and VO^+ ($^1\Sigma/^3\Sigma$); formation of propynaldehyde and the moiety V-$(OH_2)^+$; and two elimination processes of water molecule to yield cationic products, Prod-fc$^+$ and Prod-dc$^+$ where the vanadium atom adopts a four- and di-coordinate structure, respectively.

1. Introduction

Gas-phase chemical reactivity involving transition metal oxides and organic compounds constitutes a challenging research topic due to the complicated nature of the reaction mechanisms involved and their key role in many recent technological applications.[1−11] In particular, the selective oxidation of unsaturated or saturated hydrocarbons is implicated in the major portion of catalytic processes,[12−14] providing a potential route to effectively transform lower hydrocarbons into value-added higher ones.[15−18] In addition, reactions of alkyne and alkene substrates with metallic centers are important in the determination of reaction mechanisms of certain enzymes such as nitrogenases.[19,20]

Vanadium oxide clusters are of special interest because solid materials are able to catalyze a broad range of reactions, such as SO_2 to SO_3 oxidation or oxidative dehydrogenation of alkanes and alkenes.[21−24] Also, many active catalysts contain vanadium oxide highly dispersed on different types of oxide support, and important advances may arise from gas-phase cluster studies. The formation of charged vanadium oxide clusters and their reactivity with various compounds such as hydrocarbons, alkyl halides, or alcohols have been object of numerous experimental and theoretical studies.[10,11,25−45] However, the difficulties of an experimental determination of their geometries, together with the lack of reliable thermochemical data, limit a complete understanding of the chemical reactivity involving these clusters. Quantum chemical calculations, particularly methods based on density functional theory (DFT), have raised a powerful tool to provide new insights into elementary steps, type of intermediates, reactivity patterns, and determination of electronic structure along the possible reactive channels.[40,41,43−62] Accurate theoretical computations provide an alternative source of information, allowing a very helpful interplay between theory and experiment in this area of research, as has been recently pointed out by Schwarz and co-workers.[41,63−66] Also, Mercero et al.[67] and Russo and co-workers[68−72] have stressed the importance of widely used quantum chemical calculations to illustrate spin-forbidden processes in gas-phase ion−molecule reactions, while Harvey[73] in a very recent paper shed light on the kinetics of spin-forbidden chemical reactions.

In the framework of a more extended project aiming to understand the reactions of vanadium oxide cluster cations with hydrocarbons, such as alkanes and alkenes, in three recent papers we have presented DFT studies on the mechanism of the gas-phase reactions between VO_2^+ ($^1A_1/^3A''$) and ethene,[74] ethane,[75] and propene.[76] In these cases the products of oxidation or dehydrogenation reactions possess different spin states than the reactants; that is, the reactant presents a singlet (s) spin multiplicity, VO_2^+ ($^1A_1$), while the product has a ground-state triplet (t) spin multiplicity, VO^+ ($^3\Sigma$). Therefore, a change of spin multiplicity must take place at some point along the course of these reactions and it is mandatory to determine the lowest crossing point (CP) at which the two energy surfaces of different spin intersect, determining the most likely place where the transition occurs.[77−80]

In this work the first detailed DFT analysis on the mechanism of the gas-phase reactions of VO_2^+ ($^1A_1/^3A''$) with propyne C_3H_4 (^1A) is reported. This reaction presents a new case of selective oxidation of an unsaturated hydrocarbon which has not been measured so far. In addition, it can be considered as a model system for oxidation catalysis at molecular level and as one of the varied physicochemical processes taking place in gas-phase reactivity. The objective of the present article is 3-fold: (i) provide mechanistic details of the possible reaction pathways,

* Corresponding author: phone +34 964 728083; fax +34 964728066; e-mail andres@qfa.uji.es.
[†] Universitat Jaume I.
[‡] Universidade Estadual.

10.1021/jp7109548 CCC: $40.75
Published on Web 02/06/2008

(ii) analyze the potential energy surfaces (PESs) and their crossing and clarify the dominant product channels, and (iii) the conclusions that are drawn in this article may be helpful to resolve the questions mentioned above and to highlight the interesting help that theoretical calculations can bring in future experiments.

The layout of the paper is as follows: computing methods and model systems are summarized in section 2. In section 3, an overview of the stationary points as well as the CPs along the free energy profiles are presented, analyzed, and discussed. Finally, the main conclusions are given in section 4.

2. Computing Methods and Model Systems

All calculations were performed with the Gaussian 03 (G03)-package.[81] The popular B3LYP functional[82−84] combined with the all-electron 6-311G(2d,p)[85] basis set was used for structural optimization in all reactants, products, intermediates, transition structures (TSs), and CPs involved. The unrestricted formalism is employed for the calculation of open-shell species. In order to ensure the stability of the wavefunction of the singlet species, the orbital constraint applied to the α and β sets is lifted by performing calculations with the "stable" keyword as implemented in G03, allowing the reoptimization of the wavefunction if an instability is found. The nature of the stationary points (minima and TSs) has been characterized by analysis of the vibrational normal modes. The TSs have been connected to the corresponding minima by following the minimum energy paths via the intrinsic reaction coordinate (IRC) method. Gibbs free energies were calculated at standard temperature (298.15 K) and pressure (1 atm). The natural population analysis has been made by use of the natural bond orbital (NBO) method[86,87] as implemented in G03.

The concept of minimum energy crossing point (MECP) on the seam line corresponding to the intersection between two electronic surfaces of different spin multiplicities has been used to localize and characterize the CPs. Starting from the TS closest to the crossing seams, the reaction pathway was traced down to the corresponding minimum. Thereafter, single-point calculations with the other spin multiplicity were carried out on each point along the IRC path. Consequently, we obtain the CPs as the structures that have identical geometry and energy in the s and t states. This procedure has been used in our previous studies.[74−76] On behalf of comparison, the mathematical algorithm for MECPs developed by Harvey et al.[88] has been also employed, yielding very similar structures. Therefore, the CPs that we obtain can be considered as reasonable approximations of the MECPs between s and t hypersurfaces.

3. Results and Discussion

Five possible reaction pathways are found for the oxidation process of propyne by VO_2^+ ($^1A_1/^3A''$). Paths 1 and 3 correspond to the elimination of H_2 molecule to yield propynaldehyde and VO^+. Paths 2 and 5 render two alternative products: H_2O and Prod-fc$^+$ or propynaldehyde and V-$(OH_2)^+$. Finally, path 4 yields propynaldehyde and V-$(OH_2)^+$, or different products depending on the PES: H_2O and s-Prod-dc$^+$ in *s*-PES or H_2O and t-Prod-fc$^+$ in *t*-PES. Selected geometrical parameters of the stationary points at s and t electronic states are reported in Figure 1, panels a and b, respectively. Gibbs free energy profiles are depicted in Figure 2a for paths 1, 2 and 5 and in Figure 2b for paths 3 and 4. The geometry and total energies of the crossing points obtained from the IRC paths are presented in Figure 3. For comparison purposes, we have also used the algorithm proposed by Harvey et al.[88] for a more accurate characterization of the MECP, and the geometrical and energetical values of crossing points 1−5 are gathered in the Supporting Information.

The most stable combination of reactants corresponds to the singlet PES: s-VO_2^+ ($^1A_1$) and C_3H_4 (^1A). On the triplet PES, the combination of t-VO_2^+ ($^3A''$) and C_3H_4 (^1A) species lies 35.6 kcal/mol above the singlet state. For the products, the most stable combination is formed by t-VO^+ ($^3\Sigma$), H_2, and propynaldehyde for paths 1 and 4 and by t-Prod-fc$^+$ and H_2O for paths 2, 3, and 5. Since the spin of the ground-state reactants is different from both Prod-fc$^+$ or VO^+ products in all five reactive channels, a spin inversion process must occur via a CP along the reaction pathways.

The addition of vanadyl cation to the C(1)−C(2) triple bond of propyne is the starting point of the barrierless reaction that forms adducts s/t-1 in the s and t PES, respectively. Geometric parameters are similar to the isolated reactants except for the C(1)−C(2) distance, which is slightly elongated to 1.228 Å compared to 1.197 Å in free propyne. s-1 and t-1 complexes are more stable than the reactants asymptote by 47.0 and 47.3 kcal/mol, respectively. In s/t-1, the negative charge on the C(1) atom increases in 0.24/0.19 au (see the Supporting Information for a full list of NBO atomic charges for all species), and there is a significant electronic charge transfer of 0.27 and 0.21 au from the propyne fragment to the vanadyl moiety for s and t species, respectively.

The following step comprises the hydrogen transfer from the methyl group to one of the oxygen atoms of the vanadyl moiety via s/t-TS1 to obtain the minima s/t-2. The five-membered ring s/t-TS1 structure has one imaginary frequency of 1597i/1003i cm^{-1} that corresponds mainly to the expected movement of hydrogen detaching from the C(3) atom and moving toward O(1) atom, while the hydrogen atom being transferred is 0.37/0.33 au positively charged, respectively. The formation of s/t-2 is rather exothermic, 48.5/39.8 kcal/mol, respectively, and from these minima the O(2) atom of the vanadyl moiety is linked to the terminal H(2) atom via s/t-TS2, with the latter losing a noticeable amount of electronic charge (0.37/0.08 au). The stable calculation carried out on s-TS2 shows one negative eigenvalue, revealing the existence of a low-lying open-shell singlet state. However, the value of $\langle S^2 \rangle$ yields 0.32, indicating a small spin contamination from states of higher multiplicity. t-TS2 is 2.5 kcal/mol more stable than s-TS2, and therefore, a first crossing point CP1 (see Figure 3) between the s and t PESs is found in this region. An analysis of the energetic values and geometrical parameters of CP1 indicates that it is closer to t-2 than to s-2.

Considering s/t-3 minima, a second hydride transfer process takes place from C(3)atom to the V center. This reaction will occur via s/t-TS3 along paths 1−4. t-3 is considered to be a branching point, opening another alternative oxidation process: an intermolecular hydrogen transfer from H(3)to O(1)-atoms via t-TS8. In t-3 (15.6 kcal/mol more stable than s-3), the interaction between vanadium and C(1)−C(2) atoms is weaker than in s-3, as indicated by a longer interatomic distance (∼0.35 Å), favoring the existence of TS8 in the triplet state. The possibility that path 5 takes place along the singlet electronic state has not ruled out a priori. However, all attempts to localize a minimum and the corresponding transition structure at s state have been unsuccessful.

From s/t-3 it is necessary to overcome an activation free energy of 30.7/35.4 kcal/mol to reach s/t-TS3, characterized by a low imaginary vibrational frequency of 545i/451i cm^{-1} and small positive charges on the transferred H(3) atom of 0.07/0.03 for *s*/*t* surfaces, respectively. Once s/t-TS3 is surmounted, the reaction can evolve through paths 1 and 2, yielding s/t-4

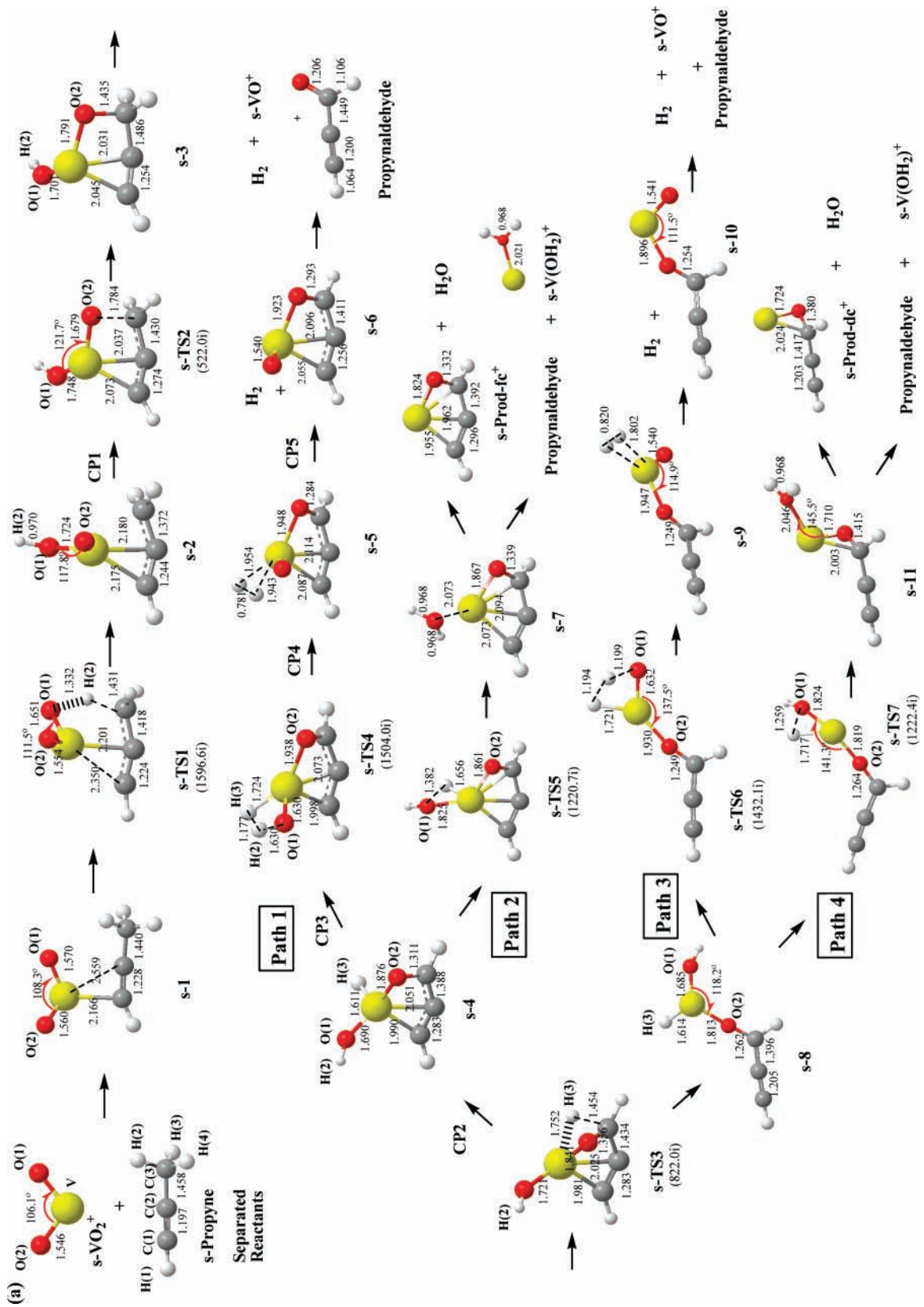

Figure 1. Part 1 of 2.

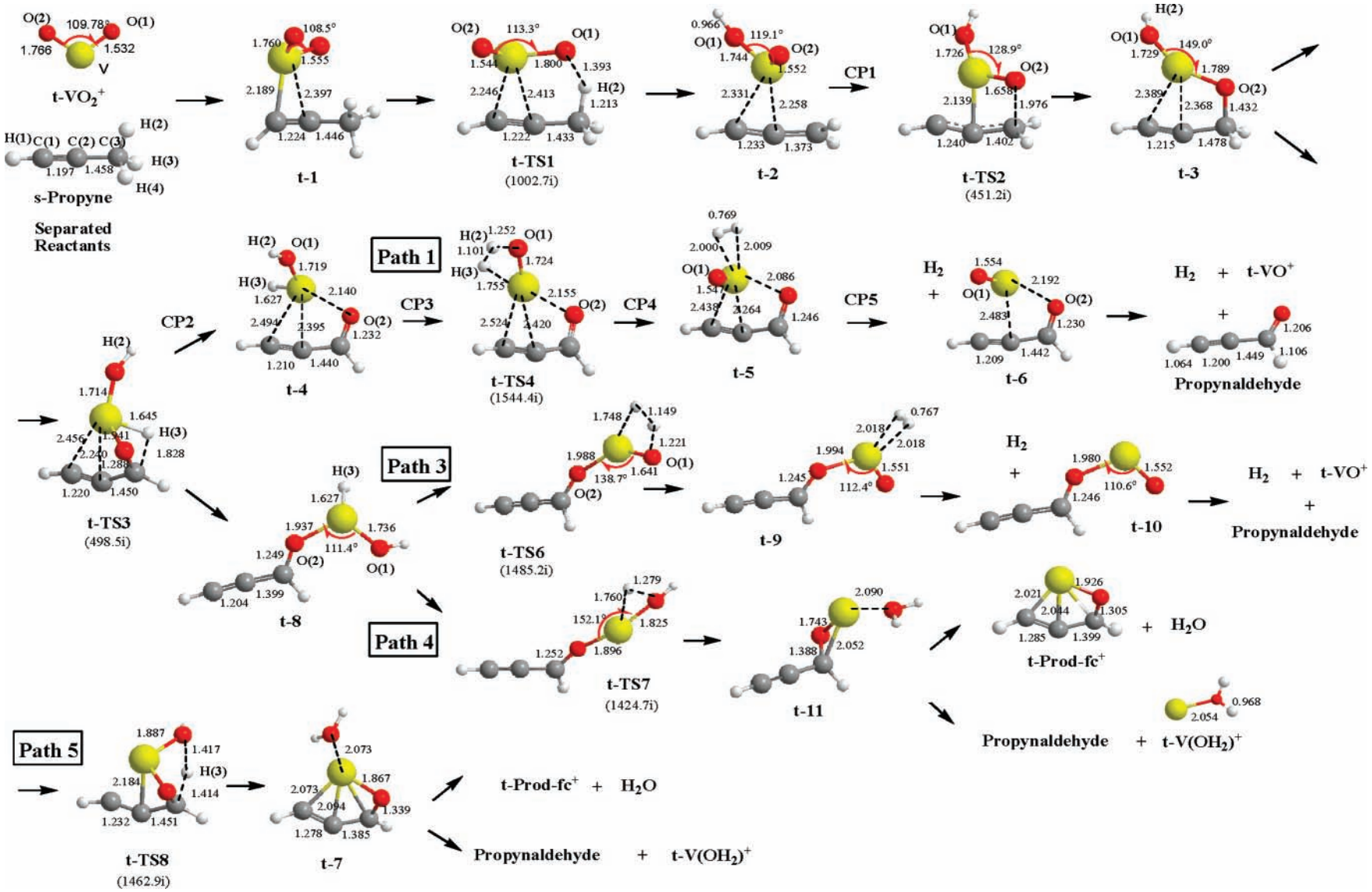

Figure 1. Structures (distances in angstroms and angles in degrees) of the stationary points found at B3LYP/6-311G(2d,p) level for (a) the singlet state and (b) the triplet state. For transition states, the imaginary vibrational frequencies (cm^{-1}) are shown in parentheses underneath.

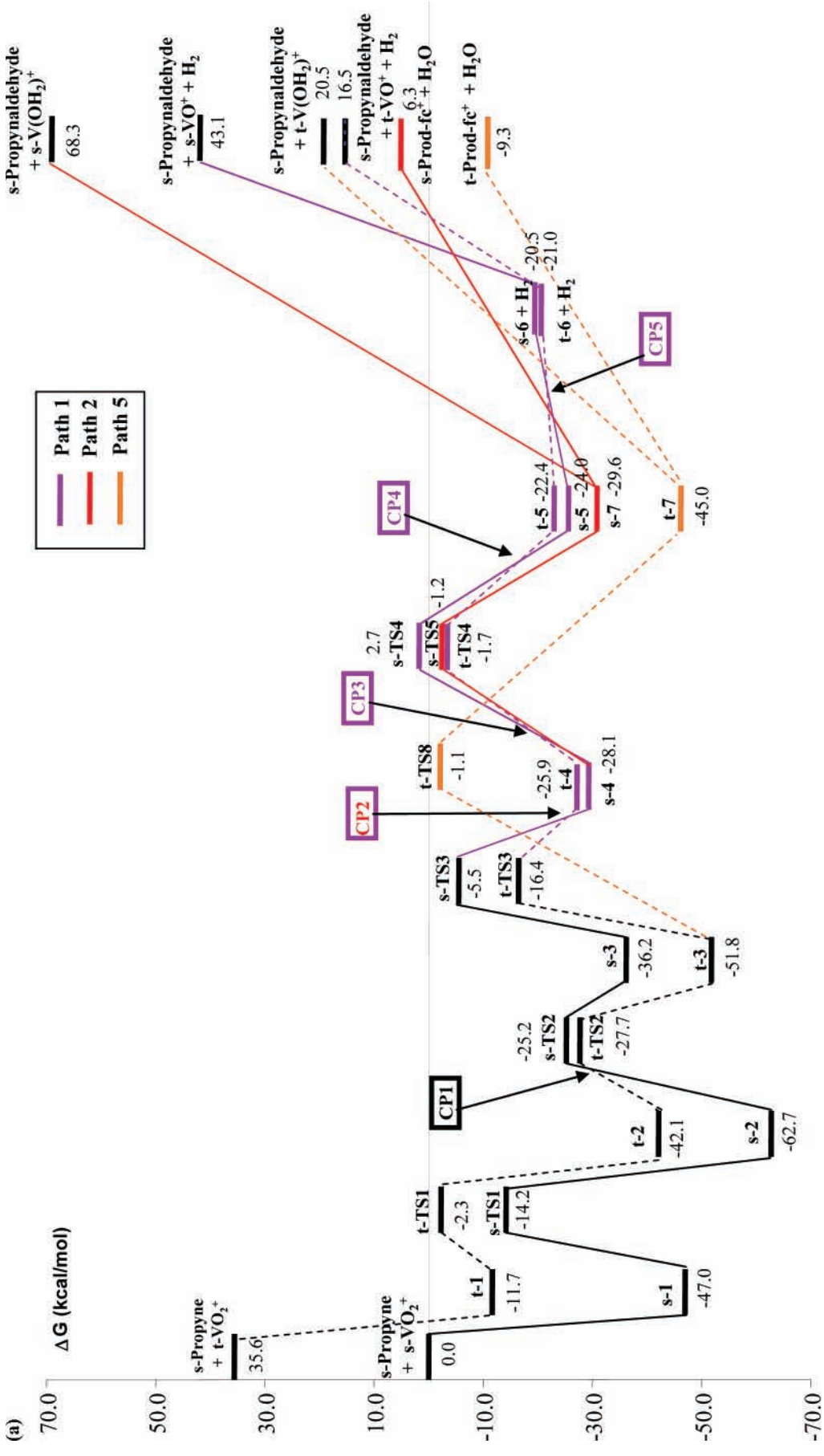

Figure 2. Part 1 of 2.

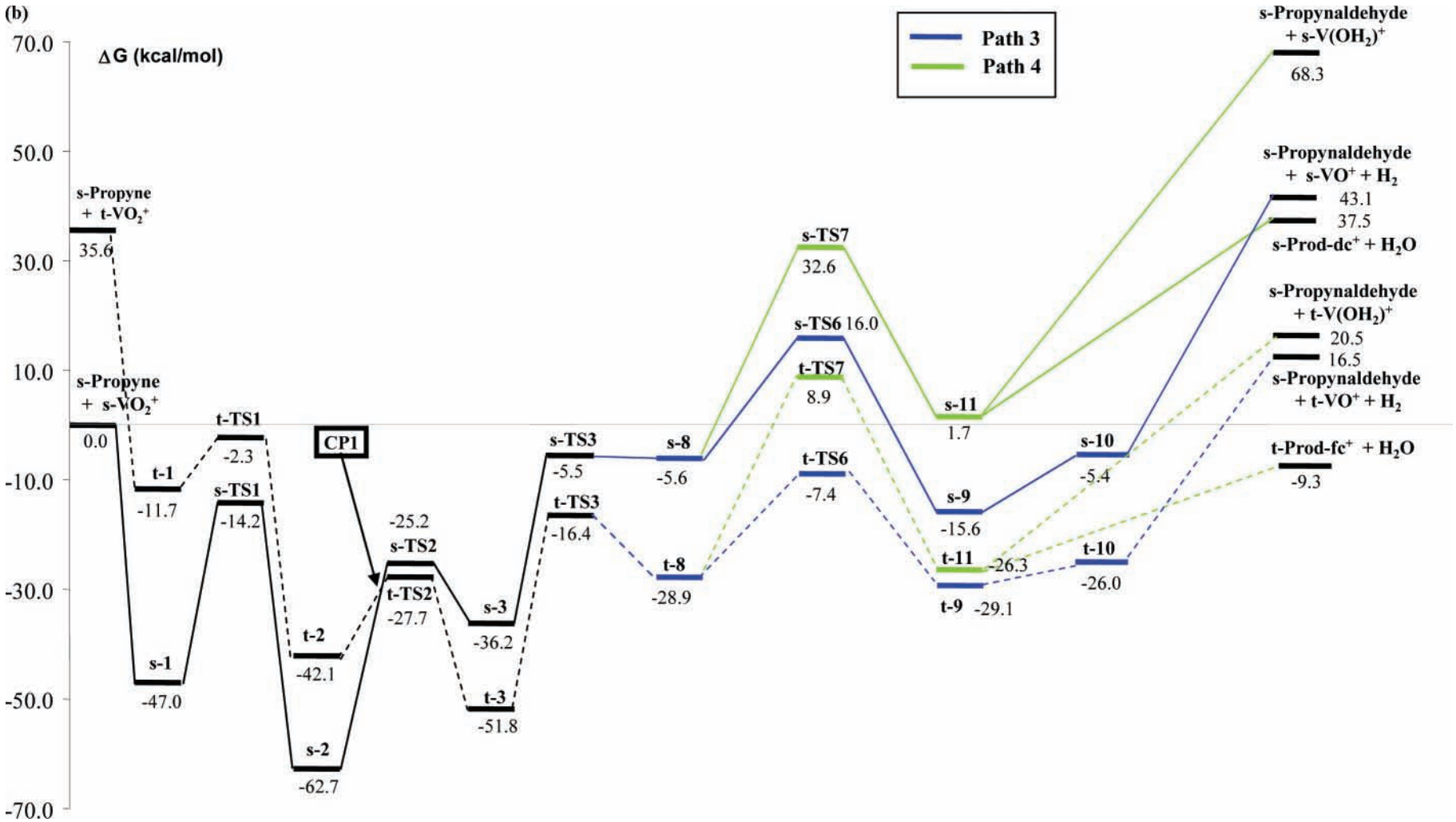

Figure 2. Gibbs free energy profiles, relative to the reactants at the singlet state. The total Gibbs free energy value for the separated reactants is −1210.857 44 hartrees at B3LYP/6-311G(2d,p) level. The singlet state is depicted with solid lines and the triplet state with dashed lines. (a) Path 1, violet; path 2, red; path 5, orange. (b) Path 3, blue; path 4, green.

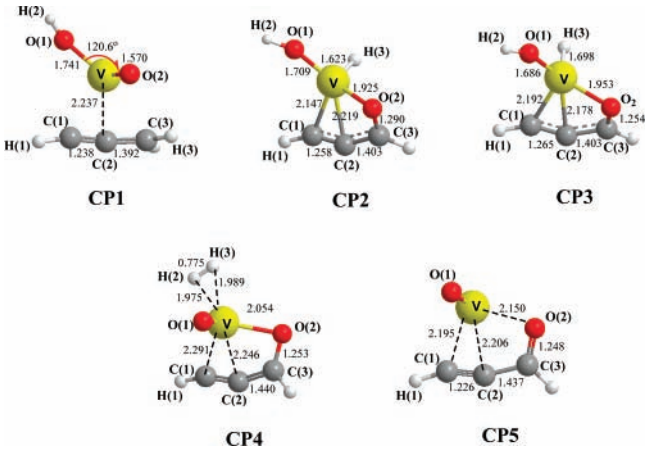

Figure 3. Structure of the crossing points, CP1, CP2, CP3, CP4 and CP5, found at B3LYP/6-311G(2d,p) level. Values of the total energies (au): CP1, −1210.951 15; CP2, −1210.917 25; CP3, −1210.913 32; CP4, −1210.914 15; CP5, −1210.886 54.

(see Figure 1a), assuming that the interaction between V and the two C atoms is preserved, or it can follow paths 3 and 4 if the V atom is detached from C(1) and C(2) atoms, to obtain s/t-8 (see Figure 2b). Therefore, at the s/t-TS3 the reaction bifurcates into two downhill pathways passing through a valley−ridge inflection point. s-4 and s/t-8 can be considered as the branching points and the order of stability order is as follows: t-8 < s-4 < t-4 < s-8. Due to the larger stability of s-4 with respect to t-4 (2.2 kcal/mol), a second spin inversion along paths 1 and 2 must occur at this stage via the CP2 point. The geometry of CP2 is depicted in Figure 3. In contrast, paths 3 and 4 remain on the triplet PES without spin crossing processes.

Path 1. Starting from s/t-4 minima, there is a hydrogen migration from the O(1) atom of the vanadyl moiety to the H(3) atom attached to vanadium. The corresponding transition structures s/t-TS4 present imaginary frequencies of 1504i/1544i cm^{-1} and the H(2)atom being transferred carries a positive charge of 0.37/0.32 au, respectively. Due to the larger stability of t-TS4 with respect to s-TS4 (4.4 kcal/mol), a third intersystem crossing (CP3) should appear on this PES region. The geometry of CP3 (see Figure 3) is very similar to that of the previous crossing point. In CP3, the distance V−H(3) has been elongated and the H(3) atom is closer to the H(2) atom compared to CP2 and also to s/t-4. s/t-5 product complexes are obtained after TS4, and the recently formed hydrogen molecule is still interacting with the vanadyl moiety. Since s-5 is 1.6 kcal/mol more stable than t-5, a fourth crossing point (CP4) appears in the region between the transition structures s/t-TS4 and s/t-5 intermediates. The geometry of CP4 is depicted in Figure 3, being geometrically and energetically closer to t-5 than to s-5.

From s/t-5 product complexes, the isolated fragments H_2 and s/t-6 can be directly obtained by overcoming a very low-energy barrier of 3.5/1.4 kcal/mol, respectively. t-6 is 0.5 kcal/mol more stable than s-6 and a fifth crossing point (CP5) is found along this step. The geometry of CP5 is shown in Figure 3, presenting geometric and energetic values intermediate between s-6 and t-6 minima. The C(1)−C(2) distance is 1.256 Å (1.209 Å) in s-6 (t-6) and 1.226 Å (1.234 Å) in CP5 (MECP). Also, the C(2)−V distance is 2.096 Å (2.483 Å) in s-6 (t-6) and 2.206 Å (2.229 Å) in CP5 (MECP). The H(4)−O(2) distance is 1.248 Å (1.238 Å) in CP5 (MECP) and 1.293 Å (1.230 Å) in s-6 (t-6). Finally, H_2 molecule, propynaldehyde, and s/t-VO^+ cations can be directly obtained from s/t-6, surmounting very large barrier heights of 63.6 and 37.5 kcal/mol, respectively.

Path 2. Starting at the s-4 intermediate, the H(3)atom attached to the V atom migrates to the O(1) atom of the vanadyl moiety via s-TS5. This displacement produces a noticeable increment of the hydrogen charge being transferred up to 0.35 au. After s-TS5, the interaction between the formed water molecule and the V atom yields the s-7 complex. From the s-7 product complex, two possible exit channels are available: (i) H_2O and a cationic product s-Prod-fc^+, in which the V atom is bounded to all three carbon atoms and the terminal oxygen atom, overcoming a barrier of 35.9 kcal/mol, or (ii) s-$V(OH_2)^+$ and propynaldehyde, surmounting a very high barrier of 97.9 kcal/mol. All the attempts carried out to localize a similar s-TS5 but in the t state have been unsuccessful.

Paths 3 and 4. These reactive channels start at s/t-8 minima and present the same type of stages as those of paths 1 and 2, respectively. Although both routes have been studied in s and t spin states (see Figure 2b), no spin crossing points have been found along these paths.

Following path 3, a transition structure (s/t-TS6) is found, as indicated by the presence of one imaginary frequency of 1432i/1485i cm^{-1}, respectively. The charge of the H(2)atom being transferred remains constant until the product complex s/t-9 is reached. From s/t-9, the isolated fragments (H_2 and s/t-10) can be directly obtained by overcoming an energy barrier of 10.2/3.1 kcal/mol, respectively. Finally, the products (H_2 molecule and s/t-VO^+ and propynaldehyde) can be directly obtained by surmounting barrier heights of 48.5 and 42.5 kcal/mol, respectively.

Reaction path 4 starts at s/t-8 minima and a transition structure (s/t-TS7) leads to the product complexes s/t-11. From s-11, two possible products can be formed: (i) H_2O and a cationic product, s-Prod-dc^+, in which the vanadium atom binds to terminal carbon and oxygen atoms and (ii) propynaldehyde and s-$V(OH_2)^+$. However, an alternative product can be obtained from t-11: H_2O and t-Prod-fc^+, in which the vanadium atom is coordinated to three carbon atoms and one oxygen atom. In t-Prod-fc^+ there is some double-bond character between C(1) and C(2) as indicated by an interatomic distance of 1.285 Å. For the s-Prod-dc^+ structure, the C(1)−C(2) distance decreases to 1.203 Å, typical of triple C−C bonds. NBO analysis shows a negative charge on C(1) of −0.35 due to its interaction with V atom.

Path 5. Starting at t-3 intermediate, an intermolecular hydrogen transfer from H(4)to O(1)atoms takes place via t-TS8, with the transferred hydrogen atom carrying a moderate positive charge of 0.14 au. This transition structure leads to the t-7 product complex, where the formed water molecule interacts with the V atom (similar to s-7 from path 2). From the t-7 complex, two possible products can be formed, H_2O and t-Prod-fc^+ by overcoming a barrier of 35.7 kcal/mol, or s-$V(OH_2)^+$ and propynaldehyde by surmounting a barrier of 65.5 kcal/mol. All the attempts carried out to characterize a similar t-TS8 but in the s state have been unsuccessful.

4. Conclusions

To gain further insight into reaction mechanism of the gas-phase ion−molecule reaction of VO_2^+ ($^1A_1/^3A''$) with propyne, an exhaustive theoretical survey on the complicated singlet and triplet PESs has been performed by means of density functional theory calculations at the B3LYP/6-311G(2d,p) level. This study provides a theoretical support for the molecular mechanisms of the title reaction, as well as thermochemical and kinetic information on the oxidation processes. Five reaction pathways have been characterized: paths 1 and 3 correspond to elimina-

tion of hydrogen molecules to yield propynaldehyde and VO^+; path 2 and path 5 render two alternative products, H_2O and Prod-fc$^+$ or propynaldehyde and V-$(OH_2)^+$; path 4 can yield propynaldehyde and V-$(OH_2)^+$, or alternative products depending on the PES, H_2O, and s-Prod-dc$^+$ in s-PES or H_2O and t-Prod-fc$^+$ in t-PES. Five crossing points between s and t electronic states have been found: CP1, which is common along all five pathways; CP2, which is common for paths 1 and 2; and the last three CPs (CP3−5), which are found along path 1.

The theoretical data obtained may thus provide a helpful tool for interpretation and prediction of the experimental findings about this reaction or similar ones and a useful guide for understanding the chemical reactivity of VO_2^+ with saturated and unsaturated hydrocarbons, as well as the mechanism of other analogous reactions. The following conclusions can be drawn:

(i) The first step of the reaction between VO_2^+ ($^1A_1/^3A''$) and propyne is a barrierless process, yielding the reactive complexes s/t-1. From these minima, a C−H bond activation process takes place, associated with a hydrogen transfer from carbon to an oxygen atom (s/t-TS1). The next step corresponds to the formation of a carbon−oxygen bond, via s/t-TS2, and the first crossing point (CP1) takes place before this transition structure is achieved. The remaining steps occur preferentially at the triplet electronic state.

(ii) From the next minima, s/t-3, a hydride transfer process takes place from H(4) to the V atoms via s/t-TS3, allowing four different reactions paths: paths 1−4. However, t-3 is considered a branching point opening another alternative oxidation process, an intermolecular hydrogen transfer from H(4)to O(1)atoms, via t-TS8, with the reaction going along path 5. From s/t-TS3 the reaction bifurcates into two equivalent downhill pathways to reach s/t-4 or s/t-8, depending on the maintenance of the interaction between V and two C carbon atoms.

(iii) The most kinetically and thermodynamically favorable reaction pathway takes place along path 5 to yield the most stable products, t-Prod-fc$^+$ and H_2O.

(iv) Along path 2, the presence of CP2 just before s/t-4 should control the outcome of the reaction to the second most stable combination of products, s-Prod-fc$^+$ and H_2O.

(v) Propynaldehyde, t-VO^+, and H_2 products provided in paths 1 and 3 are 10.2 kcal/mol above than those from path 2. Along path 3, a barrier of 21.5 kcal is overcome in the process to form the H_2 molecule. Along path 1, the corresponding barrier energy along t-PES is 27.6 kcal/mol, and there are other three spin inversion processes, CP3, CP4, and CP5, before the formation of the product complex.

Acknowledgment. This work was supported by the Ministerio de Educación y Ciencia (MEC; DGICYT, CTQ2006-15447-C02-01), Generalitat Valenciana (GV; Projects ACOMP06/122 and GV2007/106) and the Universitat Jaume I (UJI)−Fundació Bancaixa (Project P1.1B2004-20). L.G. and V.P. acknowledge GV and MEC for providing a postdoctoral grant (APOSTD07) and JdC fellowship. J.R.S. thanks the Brazilian Funding Agencies FAPESP, CAPES, CNPq, and FUNDUNESP and UJI−Fundació Bancaixa for providing a research grant. We are also grateful to the Servei d'Informatica, UJI, for generous allotment of computer time.

Supporting Information Available: Tables S1 and S2, natural population analysis of all stationary points localized for the singlet and triplet species, respectively, and Figure S1, energetic and geometrical data for MECPs of crossing points 1−5, calculated from the Harvey algorithm. This material is available free of charge via the Internet at http://pubs.acs.org.

References and Notes

(1) Fiedler, A.; Schroder, D.; Shaik, S.; Schwarz, H. *J. Am. Chem. Soc.* **1994**, *116*, 10734.
(2) Fiedler, A.; Kretzschmar, I.; Schroder, D.; Schwarz, H. *J. Am. Chem. Soc.* **1996**, *118*, 9941.
(3) Harvey, J. N.; Aschi, M. *Phys. Chem. Chem. Phys.* **1999**, *1*, 5555.
(4) Schröder, D.; Shaik, S.; Schwarz, H. *Acc. Chem. Res.* **2000**, *33*, 139.
(5) Ogliaro, F.; Harris, N.; Cohen, S.; Filatov, M.; de Visser, S. P.; Shaik, S. *J. Am. Chem. Soc.* **2000**, *122*, 8977.
(6) Zemski, K. A.; Bell, R. C.; Castleman, A. W. *J. Phys. Chem. A* **2000**, *104*, 5732.
(7) Zemski, K. A.; Justes, D. R.; Castleman, A. W. *J. Phys. Chem. A* **2001**, *105*, 10237.
(8) Oyama, S. T.; Radhakrishnan, R.; Seman, M.; Kondo, J. N.; Domen, K.; Asakura, K. *J. Phys. Chem. B* **2003**, *107*, 1845.
(9) Fielicke, A.; Meijer, G.; von Helden, G. *Eur. Phys. J. D* **2003**, *24*, 69.
(10) Justes, D. R.; Moore, N. A.; Castleman, A. W., Jr. *J. Phys. Chem. B* **2004**, *108*, 3855.
(11) Engeser, M.; Schroder, D.; Schwarz, H. *Chem.—Eur. J.* **2005**, *11*, 5975.
(12) Oyama, S. T.; Hightower, J. W. *Catalytic Selective Oxidation*; American Chemical Society: Washington, DC, 1993.
(13) Warren, B. K.; Oyama, S. T. *Heterogeneous Hydrocarbon Oxidation*; American Chemical Society: Washington, DC, 1996.
(14) Hodnett, B. K. *Heterogeneous Catalytic Oxidation*; John Wiley & Sons Ltd.: New York, 2000.
(15) Weissermel, K.; Arpe, H.-J. *Organic Synthesis by Oxidation with Metal Compounds*; Plenum: New York 1986.
(16) Bettahar, M. M.; Costentin, G.; Savary, L.; Lavalley, J. C. *Appl. Catal. A* **1996**, *145*, 1.
(17) Weissermel, K.; Arpe, H.-J. *Industrial Organic Chemistry*; VCH: Weinheim, Germany, 1997.
(18) Olah, G. A.; Molnar, A. *Hydrocarbon Chemistry*; John Wiley & Sons: Hoboken, NJ, 2003.
(19) Dance, I. *J. Am. Chem. Soc.* **2004**, *126*, 11852.
(20) Dance, I. *J. Am. Chem. Soc.* **2007**, *129*, 1076.
(21) Kung, H. H. *Transition Metal Oxides: Surface Chemistry and Catalysis, Studies in Surface Science and Catalysis*; Elsevier: Amsterdam, 1989; Vol. 45.
(22) Topsoe, N.-Y. *Science* **1994**, *265*, 1217.
(23) Haggin, J. *Chem. Eng. News* **1995**, *73*, 20.
(24) Ruth, K.; Burch, R.; Kieffer, R. *J. Catal.* **1998**, *175*, 27.
(25) Bell, R. C.; Zemski, K. A.; Kerns, K. P.; Deng, H. T.; Castleman, A. W., Jr. *J. Phys. Chem. A* **1998**, *102*, 1733.
(26) Bell, R. C.; Zemski, K. A.; Castleman, A. W., Jr. *J. Cluster Sci.* **1999**, *10*, 509.
(27) Bell, R. C.; Zemski, K. A.; Castleman, A. W., Jr. *J. Phys. Chem. A* **1999**, *103*, 2992.
(28) Foltin, M.; Stueber, G. J.; Bernstein, E. R. *J. Chem. Phys.* **1999**, *111*, 9577.
(29) Harvey, J. N.; Diefenbach, J. N.; Schröder, D.; Schwarz, H. *Int. J. Mass Spectrom.* **1999**, *182/183*, 85.
(30) Bell, R. C.; Zemski, K. A.; Justes, D. R.; Castleman, A. W., Jr. *J. Chem. Phys.* **2001**, *114*, 798.
(31) Fielicke, A.; Rademann, K. *Phys. Chem. Chem. Phys.* **2002**, *4*, 2621.
(32) Zemski, K. A.; Justes, D. R.; Castleman, A. W., Jr. *J. Phys. Chem. B* **2002**, *106*, 6136.
(33) Asmis, K. R.; Brummer, M.; Kaposta, C.; Santambrogio, G.; von Helden, G.; Meijer, G.; Rademann, K.; Woste, L. *Phys. Chem. Chem. Phys.* **2002**, *4*, 1101.
(34) Schroder, D.; Engeser, M.; Bronstrup, M.; Daniel, C.; Spandl, J.; Hartl, H. *Int. J. Mass Spectrom.* **2003**, *228*, 743.
(35) Justes, D. R.; Mitric, R.; Moore, N. A.; Bonacic-Koutecky, V.; Castleman, A. W., Jr. *J. Am. Chem. Soc.* **2003**, *125*, 6289.
(36) Justes, D. R.; Castleman, A. W., Jr.; Mitric, R.; Bonacic-Koutecky, V. *Eur. Phys. J. D* **2003**, *24*, 331.
(37) Engeser, M.; Schlangen, M.; Schroder, D.; Schwarz, H.; Yumura, T.; Yoshizawa, K. *Organometallics* **2003**, *22*, 3933.
(38) Schroder, D.; Loos, J.; Engeser, M.; Schwarz, H.; Jankowiak, H. C.; Berger, R.; Thissen, R.; Dutuit, O.; Dobler, J.; Sauer, J. *Inorg. Chem.* **2004**, *43*, 1976.
(39) Schroder, D.; Engeser, M.; Schwarz, H.; Rosenthal, E. C. E.; Dobler, J.; Sauer, J. *Inorg. Chem.* **2006**, *45*, 6235.
(40) Asmis, K. R.; Meijer, G.; Brümmer, M.; Kaposta, C.; Santambrogio, G.; L., W.; Sauer, J. *J. Chem. Phys.* **2004**, *120*, 6461.
(41) Feyel, S.; Schroder, D.; Rozanska, X.; Sauer, J.; Schwarz, H. *Angew. Chem., Int. Ed.* **2006**, *45*, 4677.
(42) Feyel, S.; Dobler, J.; Schroder, D.; Sauer, J.; Schwarz, H. *Angew. Chem., Int. Ed.* **2006**, *45*, 4681.

(43) Engeser, M.; Schroder, D.; Schwarz, H. *Eur. J. Inorg. Chem.* **2007**, 2454.
(44) Feyel, S.; Schwarz, H.; Schroder, D.; Daniel, C.; Hartl, H.; Dobler, J.; Sauer, J.; Santambrogio, G.; Woste, L.; Asmis, K. R. *ChemPhysChem* **2007**, *8*, 1640.
(45) Wang, W. G.; Wang, Z. C.; Yin, S.; He, S. G.; Ge, M. F. *Chin. J. Chem. Phys.* **2007**, *20*, 412.
(46) Vyboishchikov, S. F.; Sauer, J. *J. Phys. Chem. A* **2000**, *104*, 10913.
(47) Vyboishchikov, S. F.; Sauer, J. *J. Phys Chem. A* **2001**, *105*, 8588.
(48) Calatayud, M.; Andrés, J.; Beltrán, A.; Silvi, B. *Theor. Chem. Acc.* **2001**, *105*, 299.
(49) Calatayud, M.; Silvi, B.; Andrés, J.; Beltrán, A. *Chem. Phys. Lett.* **2001**, *333*, 493.
(50) Calatayud, M.; Andrés, J.; Beltrán, A. *J. Phys. Chem. A* **2001**, *105*, 9760.
(51) Calatayud, M.; Berski, S.; Beltrán, A.; Andrés, J. *Theor. Chem. Acc.* **2002**, *108*, 12.
(52) Jiang, N.; Zhang, D. J. *Chem. Phys. Lett.* **2002**, *366*, 253.
(53) Zhang, D. J.; Liu, C. B.; Bian, W. S. *J. Phys. Chem. A* **2003**, *107*, 8955.
(54) Zhang, D. J.; Liu, C. B.; Bi, S. W.; Yuan, S. L. *Chem.—Eur. J.* **2003**, *9*, 484.
(55) Pykavy, M.; van Wullen, C. *J. Phys. Chem. A* **2003**, *107*, 5566.
(56) Alcami, M.; Luna, A.; Mo, O.; Yanez, M.; Tortajada, J. *J. Phys. Chem. A* **2004**, *108*, 8367.
(57) Vyboishchikov, S. F. *J. Mol. Struct. THEOCHEM* **2005**, *723*, 53.
(58) Molek, K. S.; Jaeger, T. D.; Duncan, M. A. *J. Chem. Phys.* **2005**, *123*.
(59) Zhao, L. M.; Zhang, R. R.; Guo, W. Y.; Wu, S. J.; Lu, X. Q. *Chem. Phys. Lett.* **2005**, *414*, 28.
(60) Zhao, L. M.; Guo, W. Y.; Zhang, R. R.; Wu, S. J.; Lu, X. Q. *ChemPhysChem* **2006**, *7*, 1345.
(61) Feyel, S.; Scharfenberg, L.; Daniel, C.; Hartl, H.; Schroder, D.; Schwarz, H. *J. Phys. Chem. A* **2007**, *111*, 3278.
(62) Waters, T.; Wedd, A. G.; O'Hair, R. A. J. *Chem.—Eur. J.* **2007**, *13*, 8818.
(63) Schwarz, H. *Int. J. Mass Spectrom.* **2004**, *237*, 75.
(64) Schlangen, M.; Schwarz, H.; Schroder, D. *Helv. Chim. Acta* **2007**, *90*, 847.
(65) Schlangen, M.; Schwarz, H. *Angew. Chem., Int. Ed.* **2007**, *46*, 5614.
(66) Schröder, D.; Schwarz, H. *Top. Organomet. Chem.* **2007**, *22*, 1.
(67) Mercero, J. M.; Matxain, J. M.; Lopez, X.; York, D. M.; Largo, A.; Eriksson, L. A.; Ugalde, J. M. *Int. J. Mass Spectrom.* **2005**, *240*, 37.
(68) Rondinelli, F.; Russo, N.; Toscano, M. *Theor. Chem. Acc.* **2006**, *115*, 434.
(69) Rivalta, I.; Russo, N.; Sicilia, E. *J. Comput. Chem.* **2006**, *27*, 174.
(70) Leopoldini, M.; Marino, T.; Michelini, M. D.; Rivalta, I.; Russo, N.; Sicilia, E.; Toscano, M. *Theor. Chem. Acc.* **2007**, *117*, 765.
(71) Michelini, M. D.; Russo, N.; Sicilia, E. *J. Am. Chem. Soc.* **2007**, *129*, 4229.
(72) Di, Tommaso, S.; Marino, T.; Rondinelli, F.; Russo, N.; Toscano, M. *J. Chem. Theory Comput.* **2007**, *3*, 811.
(73) Harvey, J. N. *Phys. Chem. Chem. Phys.* **2007**, *9*, 331.
(74) Gracia, L.; Sambrano, J. R.; Safont, V. S.; Calatayud, M.; Beltrán, A.; Andres, J. *J. Phys. Chem. A* **2003**, *107*, 3107.
(75) Gracia, L.; Andrés, J.; Sambrano, J. R.; Safont, V. S.; Beltrán, A. *Organometallics* **2004**, *23*, 730.
(76) Gracia, L.; Sambrano, J. R.; Andrés, J.; Beltrán, A. *Organometallics* **2006**, *25*, 1643.
(77) Armentrout, P. B. *Science* **1991**, *251*, 175.
(78) Yarkony, D. R. *J. Am. Chem. Soc.* **1992**, *114*, 5406.
(79) Yarkony, D. R. *Rev. Mod. Phys.* **1996**, *68*, 985.
(80) Plattner, D. *Angew. Chem., Int. Ed.* **1999**, *38*, 82.
(81) Frisch, M. J.; Trucks, G. W.; Schlegel, H. B.; Scuseria, G. E.; Robb, M. A.; Cheeseman, J. R.; Montgomery, J. A., Jr.; Vreven, T.; Kudin, K. N.; Burant, J. C.; Millam, J. M.; Iyengar, S. S.; Tomasi, J.; Barone, V.; Mennucci, B.; Cossi, M.; Scalmani, G.; Rega, N.; Petersson, G. A.; Nakatsuji, H.; Hada, M.; Ehara, M.; Toyota, K.; Fukuda, R.; Hasegawa, J.; Ishida, M.; Nakajima, T.; Honda, Y.; Kitao, O.; Nakai, H.; Klene, M.; Li, X.; Knox, J. E.; Hratchian, H. P.; Cross, J. B.; Bakken, V.; Adamo, C.; Jaramillo, J.; Gomperts, R.; Stratmann, R. E.; Yazyev, O.; Austin, A. J.; Cammi, R.; Pomelli, C.; Ochterski, J. W.; Ayala, P. Y.; Morokuma, K.; Voth, G. A.; Salvador, P.; Dannenberg, J. J.; Zakrzewski, V. G.; Dapprich, S.; Daniels, A. D.; Strain, M. C.; Farkas, O.; Malick, D. K.; Rabuck, A. D.; Raghavachari, K.; Foresman, J. B.; Ortiz, J. V.; Cui, Q.; Baboul, A. G.; Clifford, S.; Cioslowski, J.; Stefanov, B. B.; Liu, G.; Liashenko, A.; Piskorz, P.; Komaromi, I.; Martin, R. L.; Fox, D. J.; Keith, T.; Al-Laham, M. A.; Peng, C. Y.; Nanayakkara, A.; Challacombe, M.; Gill, P. M. W.; Johnson, B.; Chen, W.; Wong, M. W.; Gonzalez, C.; Pople, J. A. *Gaussian03* (Revision B.04); Gaussian, Inc.: Pittsburgh, PA, 2003.
(82) Becke, A. D. *Phys. Rev. A* **1988**, *38*, 3098.
(83) Becke, A. D. *J. Chem. Phys.* **1993**, *98*, 5648.
(84) Lee, C. T.; Yang, W. T.; Parr, R. G. *Phys. Rev. B* **1988**, *37*, 785.
(85) Pople, J. A.; Headgordon, M.; Raghavachari, K. *J. Chem. Phys.* **1987**, *87*, 5968.
(86) Reed, A. E.; Weinstock, R. B.; Weinhold, F. *J. Chem. Phys.* **1985**, *83*, 735.
(87) Reed, A. E.; Curtiss, L. A.; Weinhold, F. *Chem. Rev.* **1988**, *88*, 899.
(88) Harvey, J. N.; Aschi, M.; Schwarz, H.; Koch, W. *Theor. Chem. Acc.* **1998**, *99*, 95.